UNSATURATED FLOW ALONG ARROYOS AND FISSURES IN THE HUECO BOLSON, TEXAS

Bridget R. Scanlon

Final Contract Report

Prepared for

Texas Low-Level Radioactive Waste Disposal Authority
Under Interagency Contract Number IAC(90-91)0268

by

Bureau of Economic Geology
W. L. Fisher, Director
The University of Texas at Austin
Austin, Texas 78713

July 1990

CONTENTS

Abstract 1

Introduction 2

Site Description 3

Methods 4

Results and Interpretation 6

Attributes of the Unsaturated Zone Beneath Arroyos 6

Attributes of the Unsaturated Zone in and Near Fissures 7

Infiltration test at fissure 8

Comparisons Between Arroyos, Fissures, Ephemeral Streams, and Interstreams 8

References 9

Figures

1. Location of study area 11

2. Cross section A–A′ in east branch of Alamo Arroyo and B–B′ in Camp Rice Arroyo 12

3. Plan view of fissure 1 and location of sampled boreholes, neutron-probe access tubes, and ponding test and cross section of fissure 1 at ponding test site 13

4. Profiles of grain size, gravimetric moisture content, water potential, and chloride concentration for borehole 75 in Camp Rice Arroyo and borehole 76 in Alamo Arroyo 14

5. Profiles of grain size, gravimetric moisture content, water potential, and chloride concentration for boreholes 68, 69, and 70 15

6. Variation in volumetric moisture content with depth and time in access tubes 65f, 66f, and 67f 16

7. Cross section of sediment texture, gravimetric moisture content, bromide concentration, and chloride concentration in soil samples collected beneath ponding surface 17

Table

1. Gravitational, water, total, and osmotic potentials, and moisture content and chloride concentration of samples from five boreholes 18

ABSTRACT

Unsaturated flow in arroyos and fissures in the Hueco Bolson of West Texas was studied to determine if downward fluxes are higher beneath these features relative to other geomorphic settings. Soil samples collected from five boreholes in two arroyos and in and adjacent to a fissure were analyzed for moisture content, water potential, and chloride content to evaluate moisture flux. In addition, three neutron-probe access tubes were installed in and adjacent to a fissure to monitor moisture content over time. A ponding test with $CaBr_2$ as a tracer was conducted at a fissure to compare moisture movement in the fracture fill with movement in the surrounding sediments.

The arroyos are floored by a shallow (≤ 2-m [≤ 6.6-ft]) layer of surficial gravel underlain by clays. Moisture content was low in the gravel (≤ 4%) and much higher in the clay (21% to 33%). Water potentials decreased with depth, which indicates a potential for downward flux. A sharp increase in chloride concentrations below the contact between the shallow gravels and deeper clays is attributed to a larger mass of water influenced by evaporation from the low-permeability clay material.

Soil texture and moisture content in the fissure were similar to that in surrounding sediments. Water potentials were close to 0 at depth in the fissure as well as in surrounding sediments and decreased toward land surface, which suggests a potential for upward liquid water flow. Chloride concentrations were approximately two orders of magnitude lower in the fissure than in the clays of the arroyos. These low chloride concentrations indicate that chloride is being flushed downward in the region of the fissures. The ponding test showed that the downward flux of chloride and bromide was greater in the fracture fill than in surrounding sediments.

Water potentials in the fissures and arroyos are higher than those found in the ephemeral stream and interstream settings, and the higher potentials are attributed to wetter conditions in the former geomorphic settings. The upward decrease in water potentials in the fissures is similar to that found in the stream/interstream settings and suggests upward liquid water movement. These

water-potential gradients contrast with those found in the arroyos, which are downward and indicate a potential for downward water movement. Chloride concentrations in the arroyos are similar to those found in the stream/interstream sediments; however, chloride concentrations in the fissure sediments are an order of magnitude lower than those in other geomorphic settings. These comparisons suggest that the downward flux of water is greater in the fissures than in other geomorphic settings.

INTRODUCTION

Although moisture flux in the unsaturated zone of arid regions has generally been considered negligible, recent work in arid systems related to radioactive waste disposal indicates that this is not true in all regions (Gee and Hillel, 1988). Conditions favorable for downward water flux include proximity to regional discharge zones where the water table is shallow and water potentials are high, such as in Soccoro, New Mexico (flux 0.7 to 3.7 mm a^{-1} [0.03 to 0.15 inch a^{-1}]) (Stephens and Knowlton, 1986). Seasonal precipitation, patterns characterized by winter precipitation when temperature and evapotranspiration are low, also favor downward flux, such as in Hanford, Washington (flux $\leq$ 60 mm a^{-1} [$\leq$ 2.4 inches a^{-1}]) (Gee and Heller, 1985). In desert regions, which generally are characterized by low moisture fluxes, higher fluxes may occur along preferred flow paths such as ephemeral stream channels. Enhanced moisture flux at the Nevada Test Site occurs in ephemeral stream channels, playas, and subsidence craters because these areas are more frequently inundated and, with the exception of the playas, are characterized by coarser grained sediments (Tyler, 1987). Vegetative cover was also found to play an important role in controlling the net downward flux at the Hanford site (Gee and Heller, 1985).

Previous work in the Hueco Bolson of West Texas evaluated moisture fluxes on the basis of physical and chemical data in ephemeral stream channels and interstream areas. Both geomorphic settings are characterized by predominantly upward water potential gradients controlled by evapotranspiration (Scanlon and others, 1990). Chemical tracer studies indicate low net

downward fluxes in the shallow (≤ 1.5-m [≤ 5-ft] depth) subsurface (Scanlon and Richter, 1990). The purpose of the present study was to determine whether higher downward fluxes occur along surface fissures and arroyos relative to other geomorphic settings.

Site Description

The study area is located in the Hueco Bolson, which is a sediment-filled basin within the Chihuahuan Desert of Texas (fig. 1). Cretaceous bedrock underlies the basin and is exposed in the Diablo Plateau, northeast of the study area. The sediments in the Hueco Bolson are approximately 200 m (656 ft) thick in the study area and consist of 140 m (460 ft) of clay with interbedded silt and sand of the Tertiary-age Fort Hancock Formation, overlain by as much as 15 m (49 ft) of predominantly coarse grained material of the Tertiary-Quaternary-age Camp Rice Formation. A discontinuous layer of caliche occurs at 1- to 2-m (3- to 6.6-ft) depth.

Arroyos to the northwest (Alamo Arroyo) and southeast (Camp Rice Arroyo) borders of the study area capture runoff from the alluvial plain and drain into the Rio Grande. The arroyo floors consist of a thin layer of gravel (≤ 2 m [≤ 6.6 ft]) that overlies the Fort Hancock clay (fig. 2a and b) (Baumgardner, 1990). Halophytic plant communities dominated by salt cedar (*Tamarix sp.*) occur along the arroyos. Ephemeral streams that lack well-defined channels (maximum relief 0.6 m [2 ft]) drain into the arroyos. The ephemeral stream channels contain grasses, localized mesquite (*Prosopis glandulosa*), and some nonvegetated areas. The streams and arroyos are generally dry except after precipitation events. With the exception of areas proximal to the arroyos, the topography is relatively flat, with slopes of less than 1% (Baumgardner, 1990).

The fissures in the study area are described in detail by Baumgardner (1990), and only a brief summary of those features related to unsaturated zone hydrology are presented in this section. The term *fissure* refers to the alignment of discontinuous surface collapse structures; the underlying extensional feature is called a fracture (fig. 3a and b). The fissures occur in topographic lows. More dense vegetation near the fissures is attributed to wetter conditions. Living plant roots

observed in the fracture reflect higher moisture contents in this zone. Three fissures were mapped in the study area (fig. 1). The dimensions of the surface collapse features are up to 1.4 m (4.6 ft) deep by 1.6 m (5.2 ft) wide. Trenches excavated at right angles to one of the fissures show that the fracture width ranges from 65 mm (2.6 inches) at 3.8-m (12.5-ft) depth to 25 mm (1 inch) at 5.6-m (18.4-ft) depth. The vertical extent of the fracture is not known because none of the trenches reached the base of the fracture. Cavities were found at the base of a gravel layer. Although fissure development in Arizona has been attributed to differential compaction of sediments related to groundwater withdrawal (Jachens and Holzer, 1979), ground-water production in the Hueco Bolson has been minimal. Lowering of base level related to the incision of the Rio Grande in the Hueco Bolson (Mullican and Senger, 1990) may have caused natural ground-water level declines that could have resulted in fissures. A number of hypotheses related to geologic controls on fissure development are examined in Baumgardner (1990).

METHODS

Physical and chemical methods were used to evaluate unsaturated flow in the fissures and arroyos. Physical methods consisted of monitoring moisture content in the field with a neutron probe. Temporal variations in moisture content are used to determine if recharge pulses are moving through the system. In addition, soil samples were collected from boreholes for laboratory determination of soil texture, moisture content, and water (matric and osmotic) potential. The direction and rate of water movement can be determined from water potential and hydraulic conductivity data. Chemical methods included measurement of chloride concentrations in soil water extracts. These procedures are described in detail in Scanlon and Richter (1990). A ponding test was conducted at a fissure to evaluate preferential flow in the fissure relative to that in surrounding sediments.

To investigate unsaturated flow in arroyos, two boreholes were drilled to a depth of 6 m (20 ft) at the base of Camp Rice (borehole 75) and Alamo Arroyos (borehole 76). Soil samples

collected from these boreholes were analyzed in the laboratory for grain size, gravimetric moisture content, and water potential. Water potential was measured in the laboratory with the Decagon thermocouple psychrometer SC-10 sample changer.

Soil samples collected from three boreholes (68, 69, and 70) in the area of the fissures (fig. 3a) were analyzed for soil texture, gravimetric moisture content, and water potential. In addition, moisture content was monitored in the field in three neutron-probe access tubes (65f, 66f, and 67f) drilled near the other three boreholes (fig. 3a). One access tube was installed in the fissure; the other two access tubes were placed at distances of 10 and 20 m (33 and 66 ft) at right angles to the general trend of the fissure. The boreholes (58-mm [2.3-inch] diameter) were drilled with an air rotary rig, and steel drill pipe (70-mm [2.8-inch] O.D.) was used as access tubing. Moisture content was logged monthly at 0.1-m intervals from a depth of 0.3 to 6 m (1 to 20 ft). The neutron probe was calibrated with the steel casing according to procedures outlined in Scanlon (1990).

Chemical methods included analysis of chloride concentrations in soil samples collected in the arroyos and in the fissure area to obtain a qualitative estimate of the flux through the unsaturated zone. Chloride concentration data were also used to estimate the osmotic component of the water potential. A ponding test was conducted in a trench that had been excavated to a depth of approximately 4 m (13 ft) at right angles to the trend of the fissure. A 4-m^2 (46-ft^2) area was ponded to a depth of 0.4 m (1.3 ft) for approximately 6 hr with water, to which bromide was added as a tracer at a concentration of 330 g/m^3. Bromide was selected because it is chemically conservative and background concentrations in interstitial water are zero. Water for the ponding test was obtained from a nearby well and had a naturally high chloride concentration (240 g/m^3). The walls of the ponded area consisted of natural sediment, and lateral flow of water from the pond was allowed. The ponding site was not instrumented with neutron-probe access tubes or soil solution samplers, to avoid introducing artificial pathways for the ponded solution. Approximately 36 hr after cessation of ponding, the ponded area was excavated with a bulldozer to a depth of 2.2 m (7 ft) below the ponded surface. Soil samples were collected at depth intervals of 0.2 to 0.4 m (0.7 to 1.3 ft) in the fracture fill and from profiles at 0.2, 0.5, 1.0, 1.5, and 2 m (0.7, 1.6,

3.3, 4.9, and 6.6 ft) parallel to the fracture. These soil samples were analyzed for grain size and moisture content. Soil-water extracts from these samples were analyzed for chloride concentration by titration and for bromide concentration by ion chromatography.

RESULTS AND INTERPRETATION

Attributes of the Unsaturated Zone Beneath Arroyos

Arroyos are floored by a shallow zone (0.3 m [1 ft]) of coarse gravel (64% to 70% gravel) that is underlain by predominantly clay-rich sediments (44% to 80% clay) (fig. 2; table 1). In sediments from borehole 76, low moisture content (2% to 4%) in the uppermost 0.5 m (1.6 ft) corresponds to that of sandy gravel material, and higher moisture content (21% to 33%) at depth corresponds to that of clay sediments (fig. 4a and b). Moisture content is more variable with depth in borehole 75 (fig. 4e); however, grain-size distribution was not analyzed for these samples.

Water potentials in the unsaturated zone beneath arroyos ranged from –0.2 MPa at the surface to –2.8 MPa at depth (fig. 4c and f; table 1). The decrease in water potentials with depth suggests a potential for downward flow. The range in water potentials was similar in both Camp Rice and Alamo Arroyo boreholes. In borehole 76, the gradient in water potentials was high beneath the contact between the surficial gravels and the underlying clays, and water potentials within the clay were relatively uniform (–2.6 to –2.8 MPa). Water potentials were more variable in samples from borehole 75.

Chloride concentrations in soil samples beneath the arroyos ranged from 50 to 4,500 mg/L (fig. 4d and g). Low chloride concentrations were recorded in the surficial gravel sediments; chloride concentrations increase sharply at the contact between the gravel and the underlying clay. High chloride concentrations in the clay are attributed to the low permeability and high porosity of these sediments, which decrease the downward water flux and allow infiltrated water to evaporate.

Attributes of the Unsaturated Zone in and Near Fissures

Soil texture in the fissure is similar to that in the adjacent area (fig. 5a, e, and i; table 1) except at 2-m (6.6-ft) depth. At 2-m (6.6-ft) depth, percent gravel is greater and percent sand is less in the fissure than in nearby boreholes. The predominant soil texture of the less than 2-mm (0.08-inch) size fraction in all three boreholes is sandy loam. There is no systematic relationship between the moisture content and the proximity of the access tube to the fissure. Gravimetric moisture content ranged from 3% to 11% in soil samples from boreholes 68, 69, and 70 (fig. 5b, f, and j). Variations in moisture content in boreholes 68 and 69 were related to soil texture—high moisture content in clay-rich material and low moisture content in gravel zones. This relationship between moisture content and texture is not well defined in soil samples collected from borehole 70. Monthly monitoring of moisture content in access tubes 65f, 66f, and 67f from October 1989 through February 1990 indicated no temporal variations in moisture content (fig. 6a, b, and c).

Water potentials measured in the fissure ranged from –8.2 MPa near the surface to –0.2 MPa at depth (fig. 5c, g, and k; table 1). The higher value may not be very precise because this value is close to the upper measurement limit of the thermocouple psychrometer. The increase in water potential with depth suggests a potential for upward flow. Near-surface water potentials decreased from –8 MPa at the fissure to –10 MPa at a distance of 10 m (33 ft), and to –12 MPa at 20 m (66 ft) from the fissure.

The preponding chloride profile in the fissure is characterized by low concentrations (<100 mg/L), similar to concentrations of chloride profiles in adjacent boreholes 69 and 70 (fig. 5d, h, and l). The chloride concentrations generally decrease with depth. The low chloride concentrations indicate that chloride is being flushed downward in the region of the fissures.

Infiltration Test at Fissure

Soil texture in the fracture fill is similar to that in nearby sediments (fig. 7a). Gravimetric moisture content after the infiltration test was generally high throughout the sampled zone of the fracture fill and ranged from 0.16 to 0.29 g g^{-1} (fig. 7b) A zone of low moisture content (0.04 to 0.06 g g^{-1}) at a depth of 0.7 to 0.9 m (2.3 to 3 ft) corresponded to a gravel-rich layer. Water apparently flowed preferentially in the fracture fill relative to the surrounding sediments. The excavation depth of 2.2 m (7.2 ft) below the ponding surface was not sufficient to reach the base of the wetting front in the fracture fill; however, the wetting front only penetrated to a depth of approximately 1.4 m (4.6 ft) in the adjacent material.

Soil-water bromide concentrations were high in the fracture fill to a depth of 2.2 m (7.2 ft), whereas bromide concentrations were close to background values at a depth of 1.4 m (4.6 ft) in adjacent sediments (fig. 7c). Although the ponded area extended to a distance of 1 m (3 ft) from the fracture, high bromide concentrations were measured in soil-water samples collected at 1.5 m (4.9 ft) from the fracture. The profile at 2 m (6.6 ft) from the fracture fill had no bromide. Bromide data indicate that the lateral movement of the infiltrated water in the coarse-grained material at a depth of 0.7 to 0.9 m (2.3 to 3 ft) is less than in finer grained material above and below the gravel bed. The distribution of chloride is similar to bromide, except that background chloride concentrations are not zero (fig. 7d).

Comparisons Between Arroyos, Fissures, Ephemeral Streams, and Interstreams

Soil texture in the ephemeral streams differs from that found in the arroyos in that it is characterized by a shallow zone of fine-grained material and lacks the surficial gravels found in the arroyos. There is no systematic relationship between variations in moisture content and in geomorphic setting because differences in moisture content are related to changes in soil texture

within each setting. Higher water potentials in fissures (–0.2 to –12.4 MPa) and arroyos (–0.2 to –2.8 MPa) relative to those in ephemeral stream and interstream settings (–0.1 to –16 MPa) are attributed to wetter conditions in the former geomorphic settings. The water potential gradients in the fissure sediments are similar to those in ephemeral stream and interstream sediments and indicate a potential for upward liquid water movement. The upward increase in water potential in the arroyos contrasts with the upward decrease in water potential in the other geomorphic settings and suggests a potential for downward water movement in the arroyos.

Concentrations of chloride in the area of the fissures (10 to 80 mg/L) are an order of magnitude lower than those in the other geomorphic settings. The lower chloride concentrations in the fissures are attributed to flushing of chloride in this region. Chloride concentrations in the arroyos (50 to 4,500 mg/L) are the same order of magnitude as those found in the streams and interstream (14 to 9,300 mg/L) settings. The shape of the chloride profile in the arroyos differs from that in the stream/interstream areas in that the chloride concentrations do not decrease below the peak value.

REFERENCES

Baumgardner, R. W., Jr., 1990, Geomorphology of the Hueco Bolson in the vicinity of the proposed low-level radioactive waste disposal site, Hudspeth County, Texas: The University of Texas at Austin, Bureau of Economic Geology, report prepared for the Texas Low-Level Radioactive Waste Disposal Authority under Interagency Contract Number IAC(90-91)0268, 98 p.

Gee, G. W., and Heller, P. R., 1985, Unsaturated water flow at the Hanford site: a review of literature and annotated bibliography: Richland, Washington, Pacific Northwest Laboratory, Report No. PNL-5428, 42 p.

Gee, G. W., and Hillel, D., 1988, Groundwater recharge in arid regions: review and critique of estimation methods: Hydrological Processes, v. 2, p. 255–266.

Jachens, R. C., and Holzer, T. L., 1979, Geophysical investigations of ground failure related to ground-water withdrawal—Picacho basin, Arizona: Ground Water, v. 17, p. 574–585.

Mullican, W. F., III, and Senger, R. K., 1990, Hydrologic characterization of ground-water resources in south-central Hudspeth County, Texas: The University of Texas at Austin, Bureau of Economic Geology, report prepared for the Texas Low-Level Radioactive Waste Disposal Authority under Interagency Contract Number IAC(90-91)0268, 88 p.

Scanlon, B. R., and Richter, B. C., 1990, Analysis of unsaturated flow based on chemical tracers (chloride, ^{36}Cl, ^{3}H, and bromide) and comparison with physical data, Chihuahuan Desert, Texas: The University of Texas at Austin, Bureau of Economic Geology, report prepared for the Texas Low-Level Radioactive Waste Disposal Authority under Interagency Contract Number IAC(90-91)0268, 58 p.

Scanlon, B. R., Wang, F. P., and Richter, B. C., 1990, Analysis of unsaturated flow based on physical data related to low-level radioactive waste disposal, Chihuahuan Desert, Texas: The University of Texas at Austin, Bureau of Economic Geology, report prepared for the Texas Low-Level Radioactive Waste Disposal Authority under Interagency Contract Number IAC(90-91)0268, 102 p.

Stephens, D. B., and Knowlton, R. J., 1986, Soil water movement and recharge through sand at a semiarid site in New Mexico: Water Resources Research, v. 22, p. 881–889.

Tyler, S. W., 1987, Review of soil moisture flux studies at the Nevada Test Site, Nye County, Nevada: Water Resources Center, Desert Research System, University of Nevada System, Report No. 45058, 48 p.

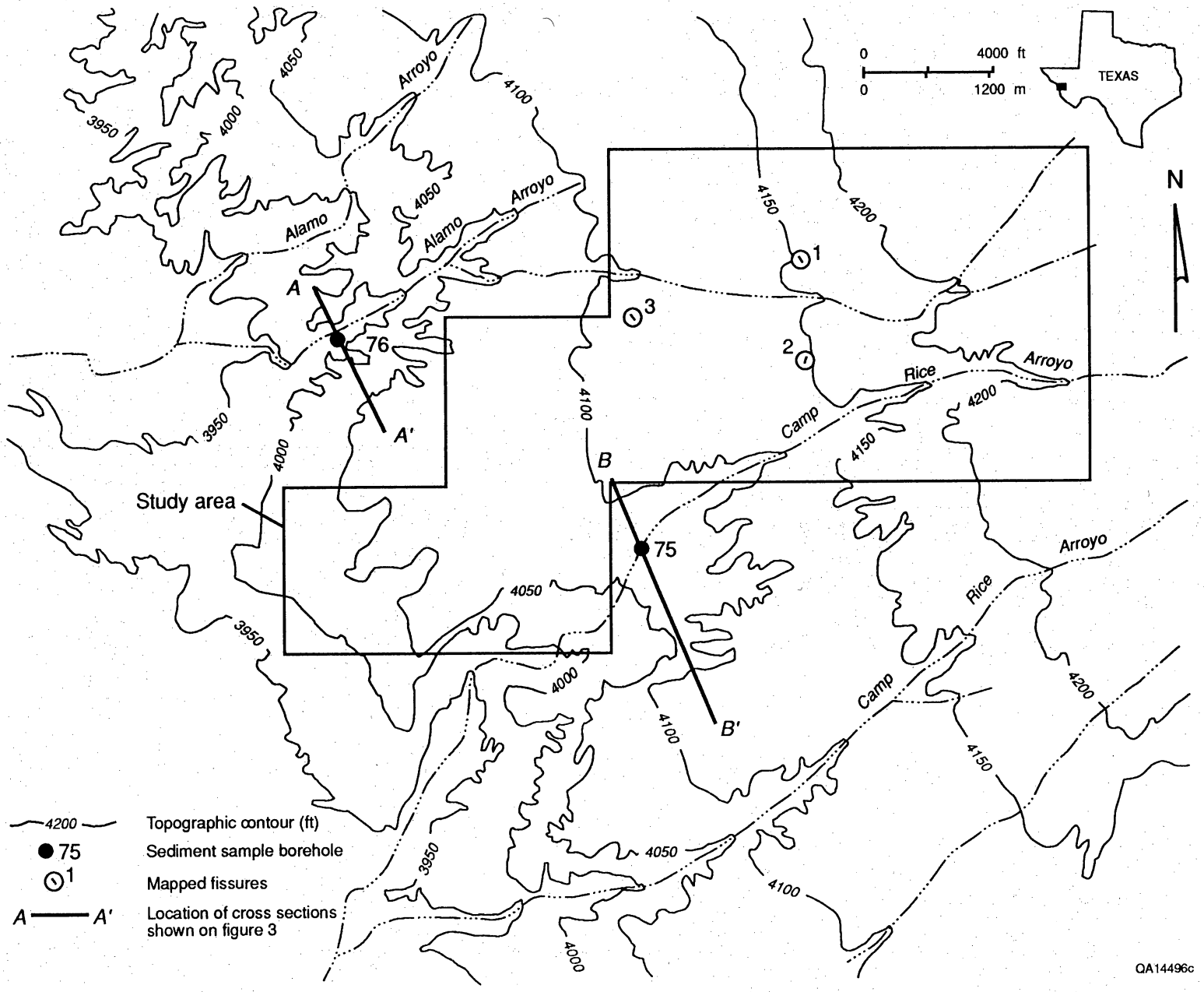

Figure 1. Location of study area. Sections A–A′ and B–B′ are shown in figure 2. Three fissure locations are labeled 1, 2, and 3.

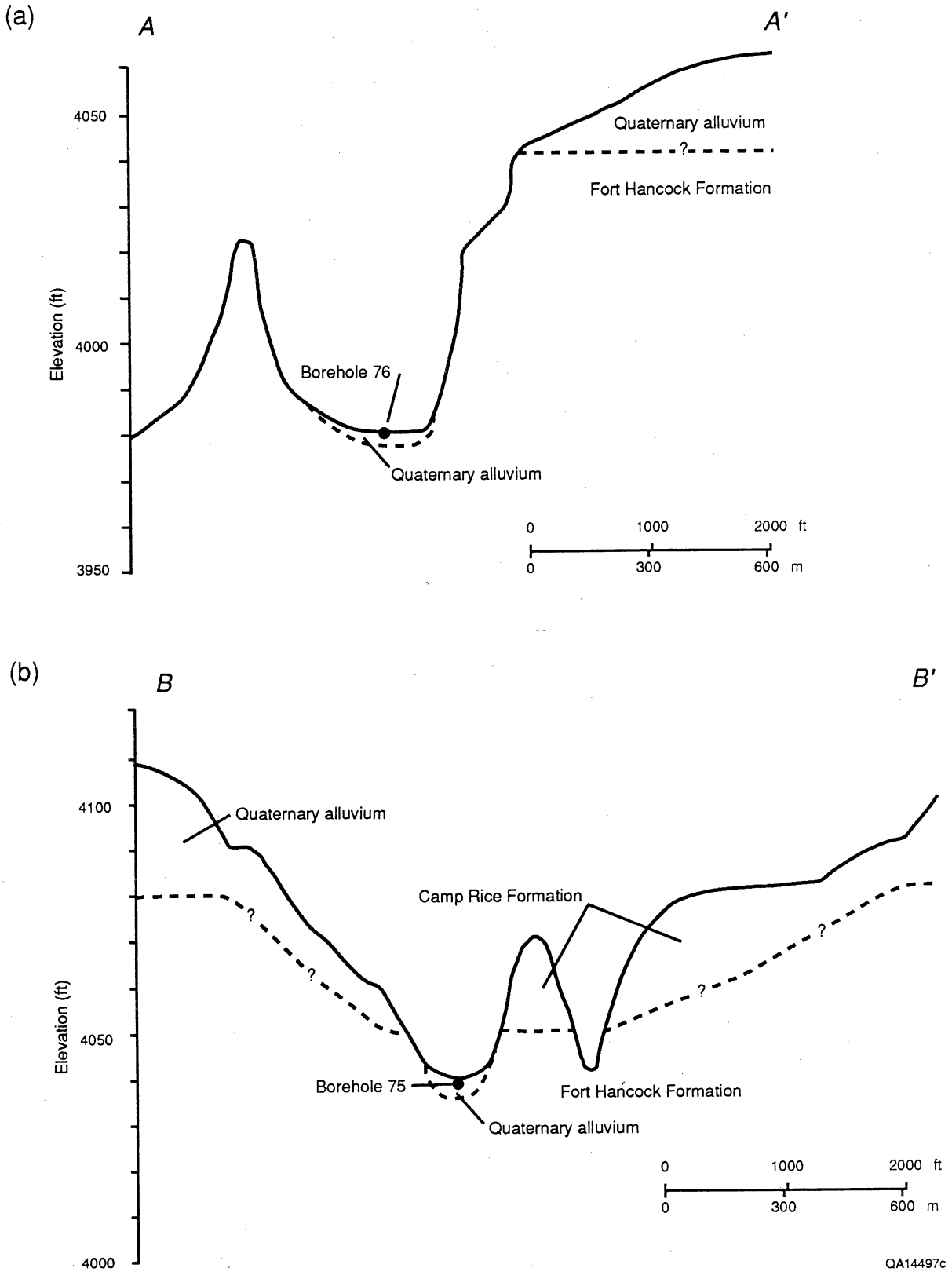

Figure 2. (a) Cross section A–A′ in east branch of Alamo Arroyo and (b) B–B′ in Camp Rice Arroyo. For location of cross sections, see figure 1.

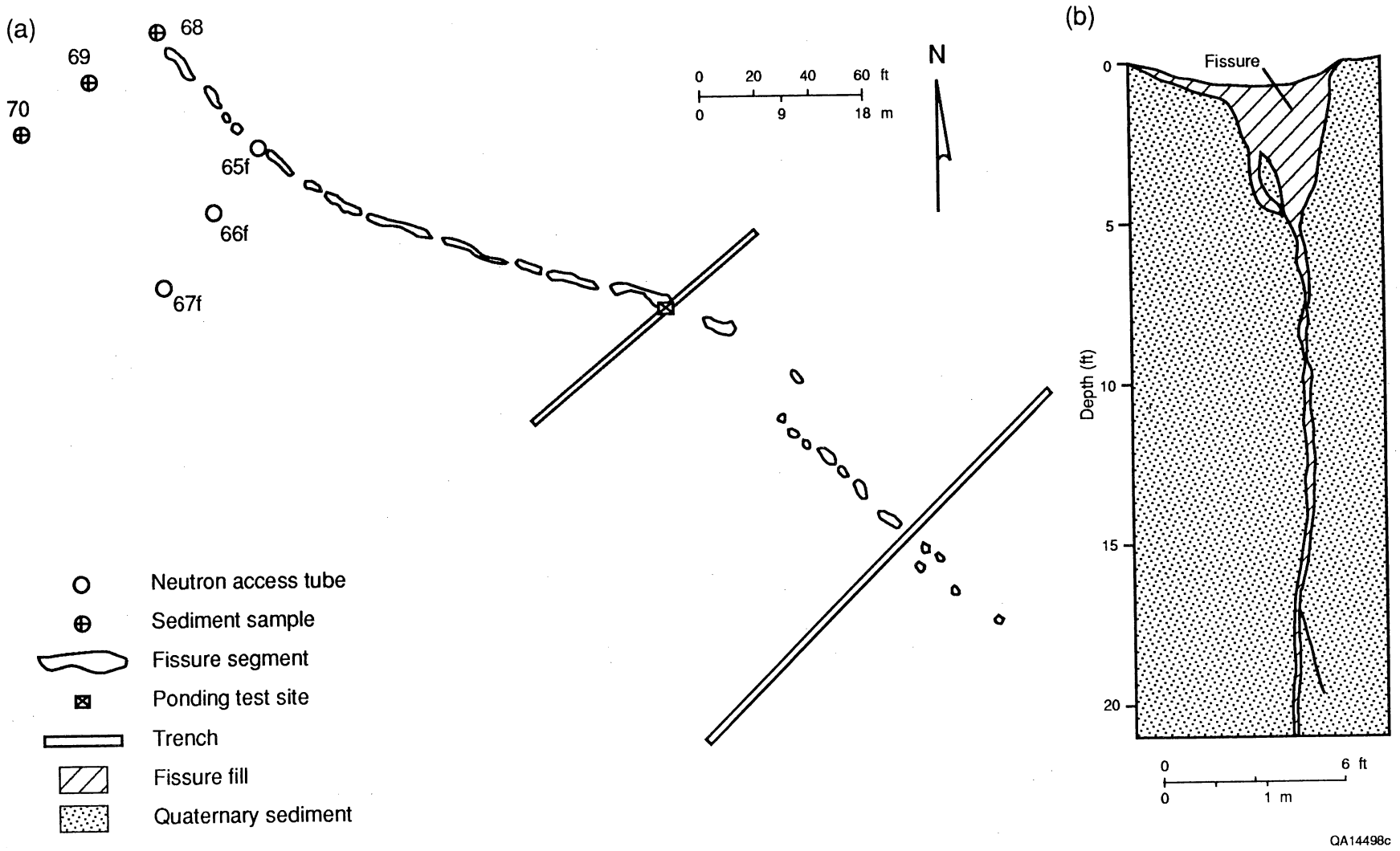

Figure 3. (a) Plan view of fissure 1 and location of sampled boreholes, neutron-probe access tubes, and ponding test and (b) cross section of fissure 1 at the ponding test site. For location of fissure 1, see figure 1.

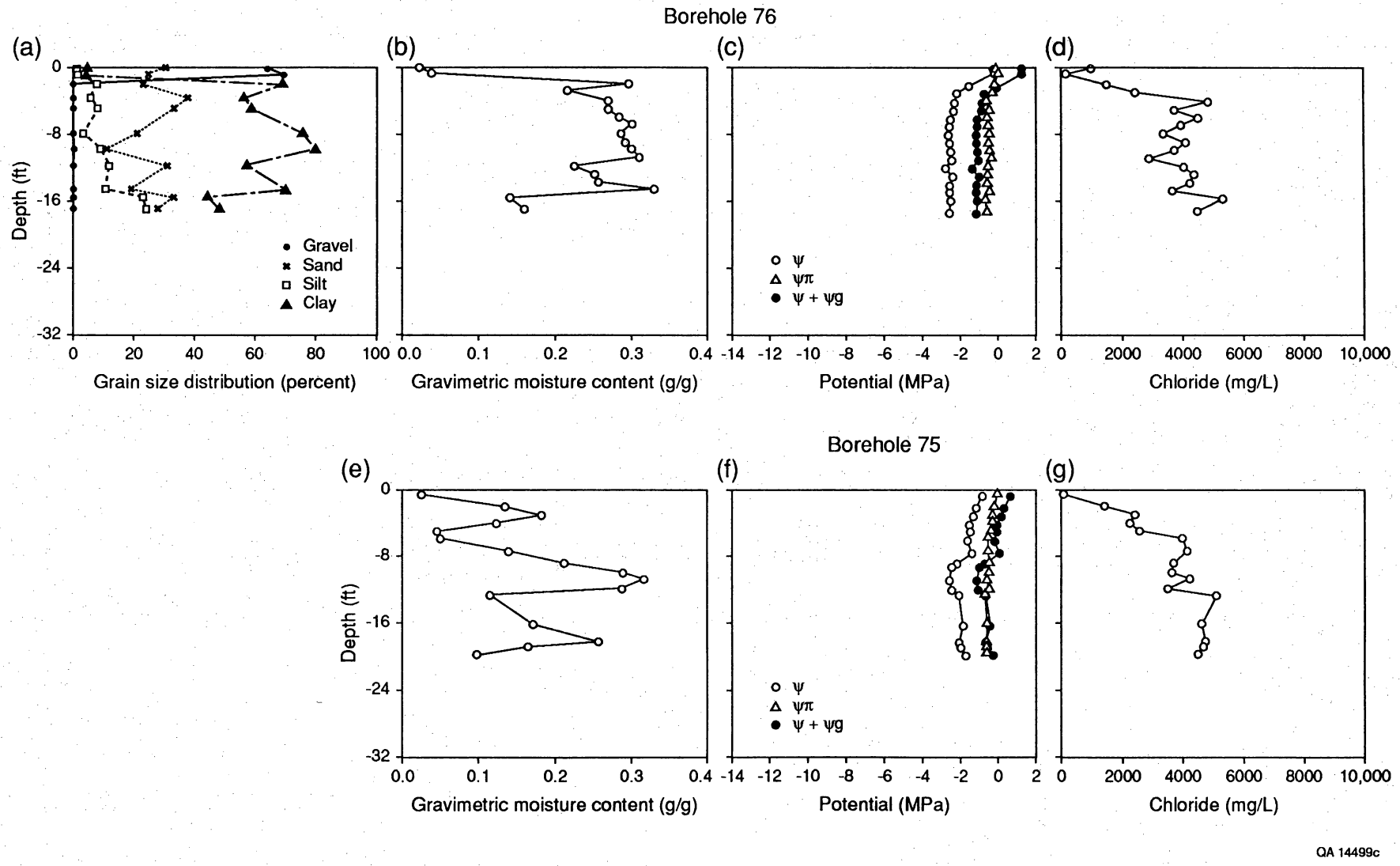

Figure 4. Profiles of grain size, gravimetric moisture content, water potential, and chloride concentration for borehole 75 in Camp Rice Arroyo and borehole 76 in Alamo Arroyo. For location of boreholes, see figure 1.

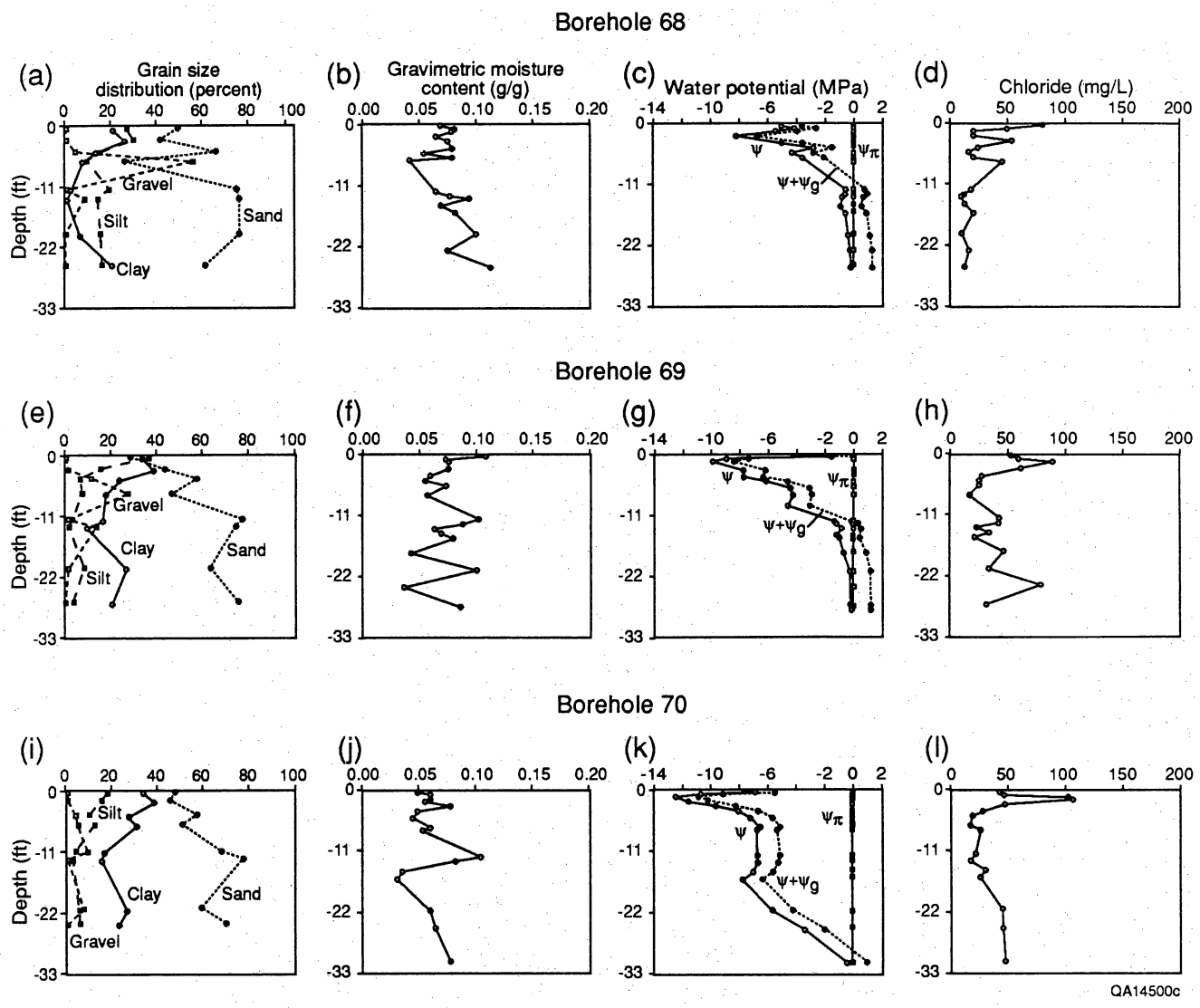

Figure 5. Profiles of grain size, gravimetric moisture content, water potential, and chloride concentration for boreholes 68, 69, and 70. For location of boreholes, see figure 3a.

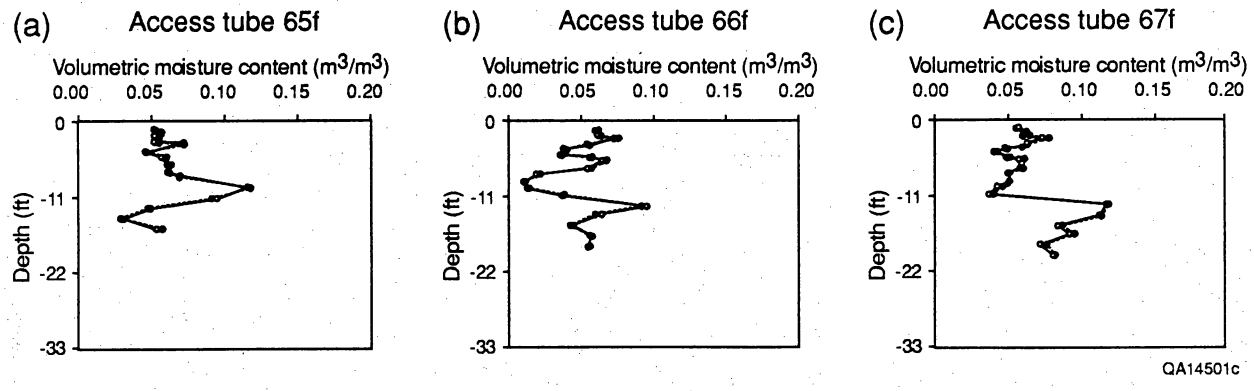

Figure 6. Variation in volumetric moisture content with depth and time in (a) access tube 65f, (b) access tube 66f, and (c) access tube 67f. Water content was monitored monthly from October 1989 through February 1990, and five curves are represented. The monitoring interval was 0.1 m (0.3 ft) from 0.3 m (1 ft) to total depth. For location of access tubes, see figure 3a.

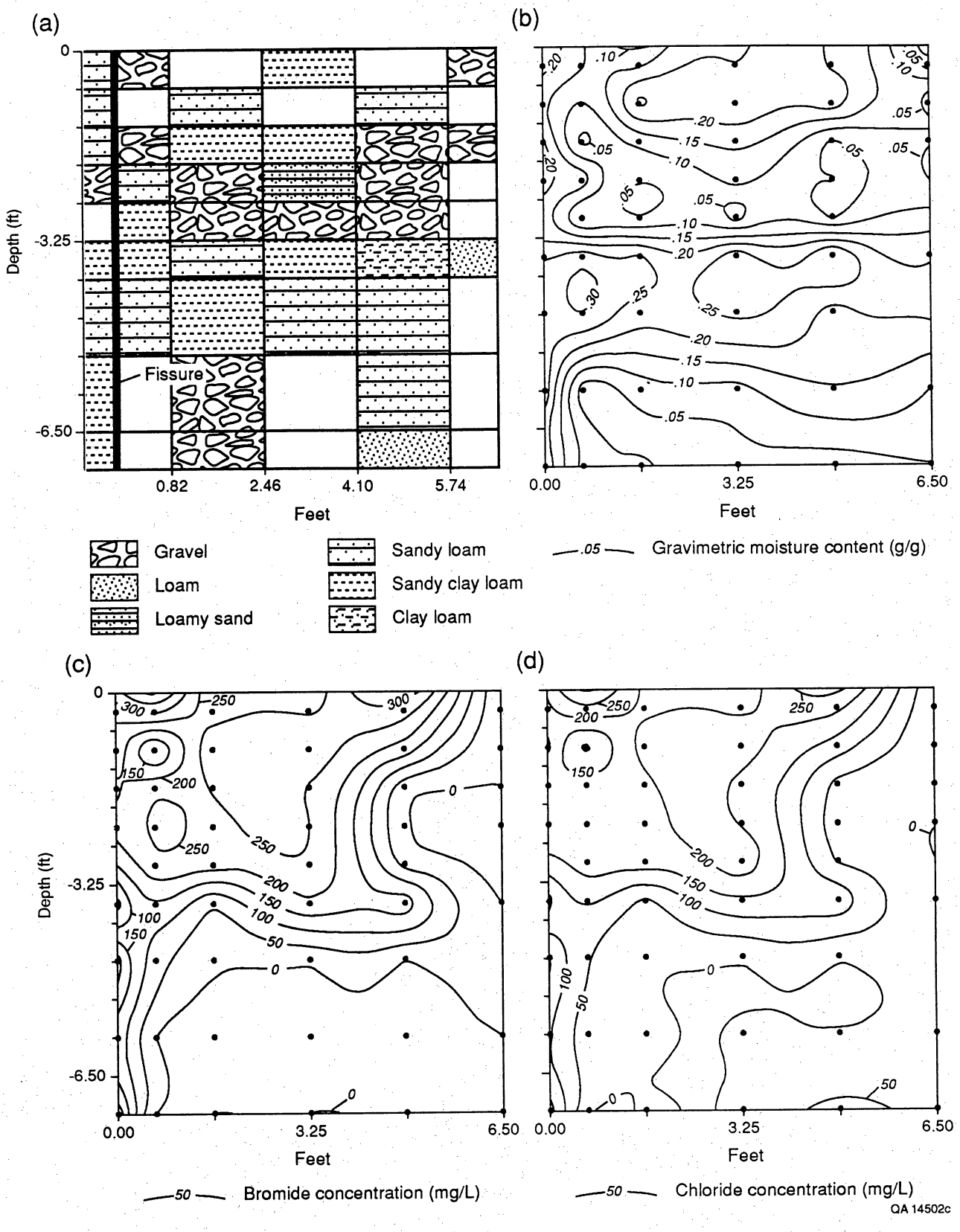

Figure 7. Cross section of (a) sediment texture, (b) gravimetric moisture content, (c) bromide concentration, and (d) chloride concentration in soil samples collected beneath ponding surface.

Table 1. Gravitational, water, total, and osmotic potentials, and moisture content and chloride concentration of samples from five boreholes.

Borehole no.	Depth (m)*	Gravitational potential (MPa)	Water potential (MPa)	Total potential (MPa)	Depth (m)	Osmotic potential (MPa)	Moisture content	Cl (mg/L)
	–0.11	1.47	–5.12	–3.65	–0.05	–0.01	0.069	80
	–0.26	1.47	–4.07	–2.60	–0.20	–0.01	0.082	50
	–0.41	1.47	–5.47	–4.01	–0.35	0.00	0.080	20
	–0.72	1.46	–8.19	–6.72	–0.66	0.00	0.065	20
	–1.02	1.46	–5.05	–3.59	–0.96	–0.01	0.075	50
	–1.33	1.46	–2.92	–1.47	–1.26	0.00	0.079	20
	–1.62	1.45	–4.38	–2.93	–1.55	0.00	0.054	20
	–1.91	1.45	–3.52	–2.07	–1.84	0.00	0.080	20
68	–3.64	1.43	–0.69	0.74	–2.00	–0.01	0.041	50
	–3.92	1.43	–0.59	0.84	–3.58	0.00	0.065	20
	–4.04	1.43	–0.74	0.69	–3.86	0.00	0.078	10
	–4.53	1.43	–0.95	0.48	–3.98	0.00	0.094	10
	–4.89	1.42	–0.57	0.85	–4.41	0.00	0.068	10
	–6.08	1.41	–0.42	0.99	–4.83	0.00	0.081	20
	–6.96	1.40	–0.16	1.24	–6.02	0.00	0.100	10
	–7.82	1.39	–0.16	1.24	–6.90	0.00	0.075	20
					–7.76	0.00	0.113	10
	–0.11	1.47	–1.51	–0.04	–0.05	–0.01	0.109	50
	–0.26	1.47	–8.86	–7.39	–0.20	–0.01	0.074	60
	–0.41	1.47	–9.85	–8.38	–0.35	–0.01	0.076	90
69	–0.87	1.46	–7.64	–6.18	–0.81	–0.01	0.075	60
	–1.17	1.46	–7.75	–6.29	–1.11	0.00	0.060	30
	–1.48	1.46	–6.12	–4.67	–1.42	0.00	0.055	30
	–1.78	1.45	–4.50	–3.04	–1.72	0.00	0.073	30

Table 1 (cont.)

Borehole no.	Depth (m)*	Gravitational potential (MPa)	Water potential (MPa)	Total potential (MPa)	Depth (m)	Osmotic potential (MPa)	Moisture content	Cl (mg/L)
	–2.24	1.45	–4.34	–2.89	–2.18	0.00	0.058	20
	–2.77	1.44	–4.58	–3.13	–3.55	–0.01	0.102	40
	–3.61	1.44	–1.46	–0.03	–3.76	–0.01	0.087	40
	–3.83	1.43	–1.17	0.26	–4.01	0.00	0.063	20
	–4.07	1.43	–0.93	0.51	–4.34	0.00	0.070	30
69	–4.40	1.43	–1.29	0.13	–4.50	0.00	0.079	20
	–4.53	1.43	–1.10	0.33	–5.30	–0.01	0.042	50
	–5.32	1.42	–0.69	0.73	–6.29	0.00	0.100	30
	–6.36	1.41	–0.29	1.12	–7.15	–0.01	0.036	80
	–8.18	1.39	–0.19	1.20	–8.12	0.00	0.085	30
	–8.40	1.39	–0.25	1.13				00
	–0.11	1.47	–6.89	–5.42	–0.05	–0.01	0.050	40
	–0.26	1.47	–10.68	–9.21	–0.20	–0.01	0.061	50
	–0.41	1.47	–12.39	–10.93	–0.35	–0.01	0.060	100
	–0.62	1.46	–11.63	–10.17	–0.56	–0.01	0.055	110
	–0.87	1.46	–9.68	–8.21	–0.81	–0.01	0.078	50
	–1.17	1.46	–8.10	–6.64	–1.11	0.00	0.050	30
	–1.48	1.46	–7.15	–5.70	–1.42	0.00	0.045	20
70	–2.03	1.45	–6.50	–5.05	–1.97	0.00	0.060	20
	–2.23	1.45	–6.67	–5.22	–2.16	0.00	0.053	20
	–3.60	1.44	–6.63	–5.19	–3.54	0.00	0.105	20
	–3.92	1.43	–6.70	–5.26	–3.87	0.00	0.083	20
	–4.48	1.43	–7.02	–5.59	–4.42	0.00	0.035	30
	–4.82	1.42	–7.80	–6.37	–4.75	0.00	0.031	30
	–6.58	1.41	–5.59	–4.18	–6.52	–0.01	0.060	50
	–7.54	1.40	–3.46	–2.07	–7.48	–0.01	0.064	50
	–9.40	1.38	–0.42	0.95	–9.34	–0.01	0.077	50

Table 1 (cont.)

Borehole no.	Depth (m)*	Gravitational potential (MPa)	Water potential (MPa)	Total potential (MPa)	Depth (m)	Osmotic potential (MPa)	Moisture content	Cl (mg/L)
	–0.26	1.47	–0.81	0.66	–0.19	–0.01	0.024	50
	–0.72	1.46	–1.16	0.30	–0.66	–0.18	0.134	1380
	–1.02	1.46	–1.33	0.13	–0.96	–0.31	0.182	2390
	–1.33	1.46	–1.55	–0.09	–1.26	–0.28	0.123	2210
	–1.61	1.45	–1.50	–0.05	–1.55	–0.33	0.045	2570
	–1.94	1.45	–1.64	–0.19	–1.84	–0.50	0.049	3930
	–2.39	1.45	–1.35	0.10	–2.32	–0.52	0.139	4120
	–2.82	1.44	–2.18	–0.74	–2.76	–0.46	0.211	3660
75	–2.93	1.44	–2.45	–1.01	–3.11	–0.46	0.289	3620
	–3.43	1.44	–2.57	–1.13	–3.37	–0.53	0.317	4200
	–3.77	1.43	–2.47	–1.03	–3.73	–0.44	0.288	3460
	–4.01	1.43	–2.10	–0.66	–3.95	–0.64	0.114	5100
	–5.09	1.42	–1.88	–0.46	–5.03	–0.58	0.171	4570
	–5.75	1.41	–2.07	–0.65	–5.68	–0.60	0.257	4710
	–5.93	1.41	–1.98	–0.57	–5.87	–0.59	0.164	4630
	–6.21	1.41	–1.71	–0.30	–6.14	–0.57	0.098	4470
	–0.06	1.47	–0.17	1.30	–0.03	–0.13	0.022	980
	–0.24	1.47	–0.19	1.28	–0.23	–0.02	0.039	160
	–0.69	1.46	–1.52	–0.06	–0.63	–0.19	0.298	1480
	–1.00	1.46	–2.19	–0.73	–0.94	–0.31	0.217	2410
76	–1.33	1.46	–2.29	–0.83	–1.26	–0.61	0.271	4830
	–1.63	1.45	–2.37	–0.91	–1.60	–0.47	0.271	3690
	–1.94	1.45	–2.54	–1.09	–1.87	–0.57	0.284	4510
	–2.24	1.45	–2.57	–1.12	–2.18	–0.50	0.301	3910
	–2.55	1.45	–2.61	–1.16	–2.48	–0.42	0.288	3330

Table 1 (cont.)

Borehole no.	Depth (m)*	Gravitational potential (MPa)	Water potential (MPa)	Total potential (MPa)	Depth (m)	Osmotic potential (MPa)	Moisture content	Cl (mg/L)
	–2.85	1.44	–2.59	–1.15	–2.79	–0.52	0.292	4090
	–3.16	1.44	–2.54	–1.10	–3.09	–0.47	0.301	3690
	–3.46	1.44	–2.48	–1.04	–3.40	–0.36	0.311	2850
	–3.77	1.43	–2.81	–1.37	–3.70	–0.51	0.226	4020
76	–4.07	1.43	–2.41	–0.98	–4.01	–0.55	0.251	4370
	–4.38	1.43	–2.57	–1.14	–4.31	–0.54	0.258	4230
	–4.68	1.42	–2.58	–1.15	–4.62	–0.46	0.330	3640
	–4.99	1.42	–2.53	–1.11	–4.92	–0.67	0.141	5310
	–5.45	1.42	–2.60	–1.18	–5.38	–0.57	0.160	4480

* 1 m = 3.28 ft